

# Optimizing the speckle noise for maximum efficacy of data acquisition in coherent imaging

François Chapeau-Blondeau,<sup>1</sup> David Rousseau,<sup>1,\*</sup> Solenna Blanchard,<sup>1</sup> and Denis Gindre<sup>2</sup>

<sup>1</sup>Laboratoire d'Ingénierie des Systèmes Automatisés (LISA), Université d'Angers, 62 avenue Notre Dame du Lac, 49000 Angers, France

<sup>2</sup>Laboratoire des Propriétés Optiques des Matériaux et Applications (POMA), Université d'Angers, 2 boulevard Lavoisier, 49000 Angers, France

\*Corresponding author: david.rousseau@univ-angers.fr

Received December 14, 2007; revised April 2, 2008; accepted April 3, 2008;  
posted April 7, 2008 (Doc. ID 90824); published May 13, 2008

The impact of multiplicative speckle noise on data acquisition in coherent imaging is studied. This demonstrates the possibility to optimally adjust the level of the speckle noise in order to deliberately exploit, with maximum efficacy, the saturation naturally limiting linear image sensors such as CCD cameras, for instance. This constructive action of speckle noise cooperating with saturation can be interpreted as a novel instance of stochastic resonance or a useful-noise effect. © 2008 Optical Society of America  
OCIS codes: 000.2690, 030.6140, 030.4280, 100.2000, 110.2970, 120.6150.

## 1. INTRODUCTION

In the domain of instrumentation and measurement, acquisition devices are generally linear for small inputs and saturate at large inputs. The linear part of their input–output characteristic usually sets the limit of the signal dynamic to be acquired with fidelity. In this paper, by contrast, we are going to show the possibility of a useful role of saturation: We report situations where the data acquisition is performed more efficiently when the information-carrying signal reaches the saturation level of the acquisition device than when it strictly remains located in its linear part. The beneficial role of saturation will be illustrated in the domain of optical coherent imaging. In this domain, because of very irregular spatial interference from the coherent phases, images have a grainy, noisy appearance called speckle. We will show how the level of the speckle noise can be optimally adjusted in order to maximize the benefit to be obtained from saturation of an image acquisition device. This constructive action of speckle noise cooperating with saturation will be interpreted as a new instance of the phenomenon of stochastic resonance. Stochastic resonance is a generic denomination that designates the possibility of improving the transmission or processing of an information-carrying signal by means of an increase in the level of the noise coupled to this signal. Since its introduction some twenty-five years ago in the context of climate dynamics, the phenomenon of stochastic resonance has experienced a large variety of extensions, developments, and observations in many areas of natural sciences (for overviews, see, for instance, [1,2]). In particular, occurrences of stochastic resonance have been reported in optics (for example, in [3–8]). Recently, stochastic resonance has been observed in coherent imaging with speckle noise in [8], where the possibility of a constructive action of speckle noise in the transmission of an image in a coherent imaging system is reported. For this first report in [8], the imaging sensor was purposely taken

in the elementary form of a 1-bit quantizer. The present paper proposes to extend the result of [8] by considering a characteristic more realistic at the signal acquisition level and more similar to practical imaging sensors such as CCD cameras, involving both linear and saturation parts. Other nonlinear systems with saturation have been investigated for stochastic resonance, but this was with a temporal (monodimensional) information signal and additive noise [9,10]. By contrast, the possibility of stochastic resonance with speckle noise, which is multiplicative noise, in a (bidimensional) imaging system with saturation is demonstrated here, to the best of our knowledge, for the first time.

## 2. COHERENT IMAGING SYSTEM

The input image  $S(u, v)$ , with  $(u, v)$  spatial coordinates, is formed by a distribution of gray levels characterized by the probability density  $p_S(s)$ . The speckle noise  $N(u, v)$ , characterized by the probability density  $p_N(n)$ , acts through the multiplicative coupling

$$S(u, v) \times N(u, v) = X(u, v), \quad (1)$$

so as to form the intermediate image  $X(u, v)$  corrupted by the speckle. The noisy image  $X(u, v)$  is observed by means of an acquisition device, described by the input–output memoryless characteristic  $g(\cdot)$ , delivering the output image

$$Y(u, v) = g[X(u, v)]. \quad (2)$$

We introduce similarity measures between the information-carrying input image  $S(u, v)$  and the output image  $Y(u, v)$ . One possibility is provided by the normalized cross covariance between images  $S(u, v)$  and  $Y(u, v)$ , defined as

$$C_{SY} = \frac{\langle SY \rangle - \langle S \rangle \langle Y \rangle}{\sqrt{\langle S^2 \rangle - \langle S \rangle^2} \sqrt{\langle Y^2 \rangle - \langle Y \rangle^2}}, \tag{3}$$

where  $\langle \cdot \rangle$  denotes an average over the images. The cross covariance  $C_{SY}$  is close to one when images  $S(u, v)$  and  $Y(u, v)$  carry strongly similar structures and is close to zero when the images are unrelated.

In addition, in the case where both input image  $S(x, y)$  and output image  $Y(x, y)$  take their values in the same range of gray levels, another input–output similarity measure is provided by the input–output rms error

$$Q_{SY} = \sqrt{\langle (S - Y)^2 \rangle}. \tag{4}$$

We want to investigate the impact of speckle noise on the input–output similarity measures  $C_{SY}$  and  $Q_{SY}$  characterizing the transmission of the images. For the sequel, we consider for the acquisition device the characteristic

$$g(x) = \begin{cases} 0 & \text{for } x \leq 0 \\ x & \text{for } 0 < x < \theta. \\ \theta & \text{for } x \geq \theta \end{cases} \tag{5}$$

The characteristic  $g(\cdot)$  of Eq. (5) is a standard model for many sensors or image acquisition devices, such as CCD cameras, for instance;  $g(\cdot)$  of Eq. (5) is purely linear for small input levels above zero, and it saturates for large input levels above  $\theta > 0$ . For instance,  $g(\cdot)$  of Eq. (5) offers a model for a CCD camera that will represent the input on, say, 256 levels between 0 and 255, and will saturate above 255.

Since in coherent imaging, following Eq. (1), the speckle noise  $N(u, v)$  has a multiplicative action on the input image, the level of the speckle noise plays a key role in fixing the position of the dynamics of the image  $X(u, v)$  applied onto the acquisition device  $g(\cdot)$  in relation to its linear range  $[0, \theta]$ . For a given sensor with a fixed saturation level  $\theta$ , too large a level of the multiplicative speckle noise  $N(u, v)$  may strongly saturate the acquisition, while too low a level of  $N(u, v)$  may result in a poor exploitation of the full dynamics  $[0, \theta]$  of the sensor. We will use the similarity measures  $C_{SY}$  and  $Q_{SY}$  of Eqs. (3) and (4) to quantitatively characterize the existence of an optimal level of the speckle noise in given conditions of image acquisition. Interestingly, the optimal level of speckle noise will be found to deliberately exploit the saturation in the operation of the sensor. By taking advantage of the saturation in this way, the acquisition reaches a maximum performance that cannot be achieved when the sensor is operated solely in the linear part of its response.

### 3. EVALUATION OF THE INPUT–OUTPUT SIMILARITY MEASURES

With the sensor  $g(\cdot)$  of Eq. (5), we now want to derive explicit expressions for the input–output similarity measures  $C_{SY}$  and  $Q_{SY}$  of Eqs. (3) and (4). For the computation of the output expectation  $\langle Y \rangle$ , it is to be noted that  $Y$  takes its values in  $[0, \theta]$  as a consequence of Eqs. (2) and (5). We introduce the conditional probability  $\Pr\{Y$

$\in [y, y + dy] | S = s\}$ . For the nonsaturated pixels in the output image  $Y(u, v)$ , with gray levels such that  $0 < y < \theta$ , one has

$$\begin{aligned} \Pr\{Y \in [y, y + dy] | S = s\} \\ &= \Pr\{N \in [y/s, y/s + dy/s]\} \\ &= p_N(y/s) dy/s, \end{aligned} \tag{6}$$

and for the saturated pixels of the output image  $Y(u, v)$ , with a gray level such that  $y = \theta$ , one has

$$\Pr\{Y = \theta | S = s\} = \Pr\{sN \geq \theta\} = \Pr\{N \geq \theta/s\} = 1 - F_N(\theta/s), \tag{7}$$

with the cumulative distribution function  $F_N(n) = \int_{-\infty}^n p_N(n') dn'$  of the speckle noise. This is enough to deduce the expectation  $\langle Y \rangle$  as

$$\langle Y \rangle = \int_s \int_{y=0}^{\theta} y p_N(y/s) \frac{dy}{s} p_S(s) ds + \int_s \theta [1 - F_N(\theta/s)] p_S(s) ds. \tag{8}$$

We introduce the auxiliary function  $G_N(n) = \int_0^n n' p_N(n') dn'$ , and then Eq. (8) becomes

$$\langle Y \rangle = \theta + \int_s [s G_N(\theta/s) - \theta F_N(\theta/s)] p_S(s) ds. \tag{9}$$

In a similar way, the expectation  $\langle SY \rangle$  is

$$\begin{aligned} \langle SY \rangle &= \int_s \int_{y=0}^{\theta} s y p_N(y/s) \frac{dy}{s} p_S(s) ds + \int_s s \theta [1 \\ &\quad - F_N(\theta/s)] p_S(s) ds, \end{aligned} \tag{10}$$

amounting to

$$\langle SY \rangle = \theta \langle S \rangle + \int_s [s^2 G_N(\theta/s) - \theta s F_N(\theta/s)] p_S(s) ds. \tag{11}$$

Evaluation of Eqs. (3) and (4) also requires the expectation  $\langle Y^2 \rangle$ , which is

$$\begin{aligned} \langle Y^2 \rangle &= \int_s \int_{y=0}^{\theta} y^2 p_N(y/s) \frac{dy}{s} p_S(s) ds + \int_s \theta^2 [1 \\ &\quad - F_N(\theta/s)] p_S(s) ds. \end{aligned} \tag{12}$$

And with the auxiliary function  $H_N(n) = \int_0^n n'^2 p_N(n') dn'$ , Eq. (12) becomes

$$\langle Y^2 \rangle = \theta^2 + \int_s [s^2 H_N(\theta/s) - \theta^2 F_N(\theta/s)] p_S(s) ds. \tag{13}$$

With  $\langle S \rangle = \int_s s p_S(s) ds$  and  $\langle S^2 \rangle = \int_s s^2 p_S(s) ds$ , Eqs. (9), (11), and (13) allow one to evaluate the input–output similarity measures  $C_{SY}$  and  $Q_{SY}$  of Eqs. (3) and (4) in given input conditions specified by  $p_S(s)$  and  $p_N(n)$ .

### 4. EXPONENTIAL SPECKLE NOISE

A useful probability density  $p_N(n)$  for the speckle noise  $N(u, v)$  is provided [11] by the exponential density

$$p_N(n) = \frac{1}{\sigma} \exp\left(-\frac{n}{\sigma}\right), \quad n \geq 0, \quad (14)$$

the density being zero for the negative gray levels  $n < 0$ . From Eq. (14), the parameter  $\sigma$  is both the standard deviation and the expectation  $\langle N \rangle$  of the speckle noise. Also, it follows from Eq. (14) that

$$F_N(n) = 1 - \exp\left(-\frac{n}{\sigma}\right), \quad n \geq 0, \quad (15)$$

$$\begin{aligned} G_N(n) &= \int_0^n n' p_N(n') dn' \\ &= \sigma \left[ 1 - \left(\frac{n}{\sigma} + 1\right) \exp\left(-\frac{n}{\sigma}\right) \right], \quad n \geq 0, \end{aligned} \quad (16)$$

and

$$\begin{aligned} H_N(n) &= \int_0^n n'^2 p_N(n') dn' \\ &= \sigma^2 \left\{ 2 - \left[ \left(\frac{n}{\sigma}\right)^2 + 2\frac{n}{\sigma} + 2 \right] \exp\left(-\frac{n}{\sigma}\right) \right\}, \quad n \geq 0. \end{aligned} \quad (17)$$

Then it results from Eq. (9) that

$$\langle Y \rangle = \sigma \langle S \rangle - \sigma \int_s \exp\left(-\frac{\theta}{s\sigma}\right) p_S(s) ds, \quad (18)$$

from Eq. (11) that

$$\langle SY \rangle = \sigma \langle S^2 \rangle - \sigma \int_s s^2 \exp\left(-\frac{\theta}{s\sigma}\right) p_S(s) ds, \quad (19)$$

and from Eq. (13) that

$$\langle Y^2 \rangle = 2\sigma^2 \langle S^2 \rangle - 2\sigma \int_s (\sigma s^2 + \theta s) \exp\left(-\frac{\theta}{s\sigma}\right) p_S(s) ds. \quad (20)$$

## 5. EXPONENTIAL SPECKLE NOISE WITH BINARY INPUT IMAGE

With the exponential speckle noise  $N(u, v)$ , we now choose to examine the situation of binary input images  $S(u, v)$ . This class of images represents, for instance, a basic model for images characterized by only two regions with very narrow probability density functions in each region. One can think of an object with an almost uniform gray level centered around  $I_1 \geq 0$ , standing over a background with an almost uniform gray level centered around  $I_0 \geq 0$ . Such a scene would be fairly approximated by its binary version containing only levels  $I_1$  and  $I_0$ . In addition, the simple choice of a binary input image  $S(u, v)$  with levels  $I_1$  and  $I_0$  will allow us to carry further the analytical treatment of our theoretical model. With Dirac delta functions, the probability density function associated with a binary image is

$$p_S(s) = p_1 \delta(s - I_1) + (1 - p_1) \delta(s - I_0), \quad (21)$$

where  $p_1$  is the fraction of pixels at  $I_1$  in image  $S(u, v)$ . It results from Eq. (21) that  $\langle S \rangle = p_1 I_1 + (1 - p_1) I_0$  and  $\langle S^2 \rangle = p_1 I_1^2 + (1 - p_1) I_0^2$ . One then obtains for Eq. (18)

$$\langle Y \rangle = \sigma \langle S \rangle - \sigma \left[ p_1 I_1 \exp\left(-\frac{\theta}{I_1 \sigma}\right) + (1 - p_1) I_0 \exp\left(-\frac{\theta}{I_0 \sigma}\right) \right], \quad (22)$$

for Eq. (19)

$$\begin{aligned} \langle SY \rangle &= \sigma \langle S^2 \rangle - \sigma \left[ p_1 I_1^2 \exp\left(-\frac{\theta}{I_1 \sigma}\right) \right. \\ &\quad \left. + (1 - p_1) I_0^2 \exp\left(-\frac{\theta}{I_0 \sigma}\right) \right], \end{aligned} \quad (23)$$

and for Eq. (20)

$$\begin{aligned} \langle Y^2 \rangle &= 2\sigma^2 \langle S^2 \rangle - 2\sigma \left[ p_1 (\sigma I_1^2 + \theta I_1) \exp\left(-\frac{\theta}{I_1 \sigma}\right) \right. \\ &\quad \left. + (1 - p_1) (\sigma I_0^2 + \theta I_0) \exp\left(-\frac{\theta}{I_0 \sigma}\right) \right]. \end{aligned} \quad (24)$$

Equations (22)–(24) now make possible an explicit evaluation of the input–output similarity measures  $C_{SY}$  and  $Q_{SY}$  of Eqs. (3) and (4).

Figures 1(A) and 1(B) give an illustration, showing conditions of nonmonotonic evolutions of the performance measures  $C_{SY}$  and  $Q_{SY}$ , which can be improved when the level of the speckle noise increases. Figures 1(A) and 1(B) demonstrate that the performance measures  $C_{SY}$  and  $Q_{SY}$  are maximized when the level  $\sigma$  of the speckle noise is tuned at an optimal nonzero value, which can be computed with the present theory. In practice, the level  $\sigma$  of the speckle noise can be controlled by experimentally varying the intensity of the coherent source. This way of controlling  $\sigma$  makes possible a confrontation of the theoretical and experimental evolutions for the performance measures  $C_{SY}$  and  $Q_{SY}$ . This confrontation has been performed, and the results are also presented in Figs. 1(A) and 1(B). We briefly describe the experimental setup in the following section.

## 6. EXPERIMENTAL VALIDATION

An optical version of the theoretical coherent imaging system described in Section 2 has been realized in the following way. A laser beam of tunable intensity goes through a static diffuser to create a speckle field, which illuminates a slide with calibrated transparency levels carrying the contrast of the input image  $S(u, v)$ . A lens then images the slide plane on a camera CCD matrix to produce the output image  $Y(u, v)$ . This experimental setup was used in [8] with an image acquisition device reduced to a simple 1-bit quantizer. By contrast, here the input–output characteristic of the image acquisition device presents the more realistic characteristic given by Eq. (5). A digital representation of the binary input image  $S(u, v)$  used to realize this experiment is shown in Fig. 2 (left), with the object representing an airplane surrounded by a dark

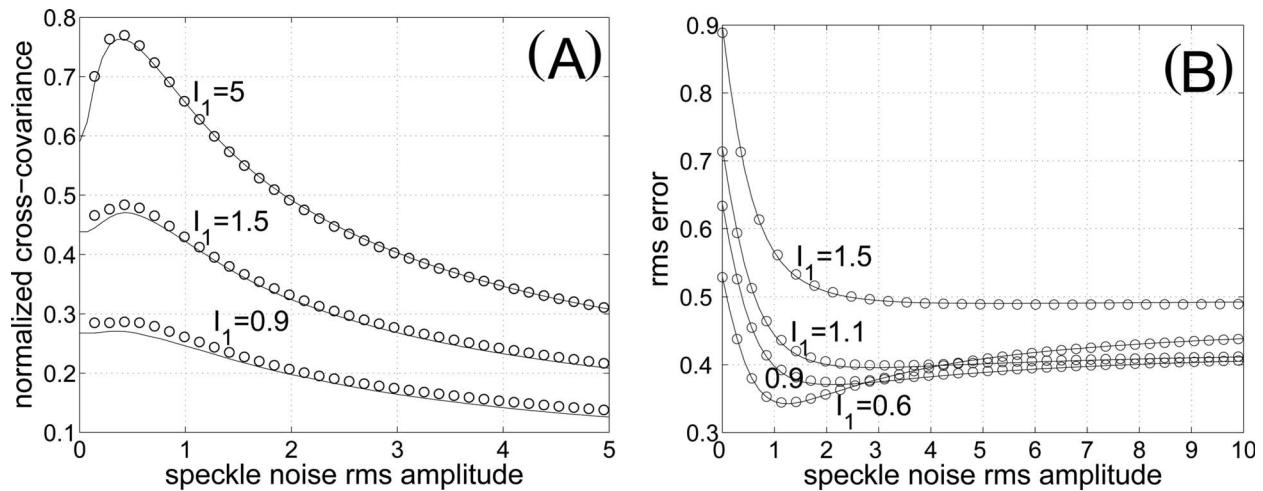


Fig. 1. Normalized cross covariance  $C_{SY}$  (A) and rms error  $Q_{SY}$  (B) as a function of the rms amplitude  $\sqrt{2}\sigma$  of the exponential speckle noise when  $\theta=1$ ,  $p_1=0.27$ , and  $I_0=0.5$  at various  $I_1$ . The solid curve stands for the theoretical expressions of Eqs. (3) and (4). The discrete data sets (circles) are obtained by injecting into Eq. (1) real speckle images collected from the experimental setup of [8].

background. Some specific conditions arise to operate the experimental setup in the domain of validity of the speckle noise model of Eqs. (1) and (14). As is visible in Fig. 2, the experimental image appears with grains typical of speckle. The probability density of Eq. (14) describes the fluctuations of gray levels in the speckle at scales below the grain size, and it does not suffer from averages over several neighboring grains [11]. As such, the speckle noise model of Eqs. (1) and (14) is adequate to describe the situation where the detector pixel size is smaller than the speckle grain size [11]. At the same time, the statistical modeling based on the probability density of Eq. (14) is meaningful if the acquired image  $Y(u, v)$  contains a large number of speckle grains for the statistics. Thus, the speckle grain size has to be controlled, like in Fig. 2 (right), in order to be much larger than the pixel size and much smaller than the CCD matrix. This control is obtained experimentally by adjusting the focus of the laser beam on the diffuser with a micrometer-scale sensitivity linear stage. Nevertheless, the speckle grain size is not a critical parameter, since it does not qualitatively affect the existence of the nonmonotonic evolution of the image acquisition performance with the speckle noise level. Quantitatively, too small a speckle grain size would

change the speckle noise probability density function, since it would result from the integration over a pixel of multiple grains. Such probability density functions would be narrower than the exponential model considered here [11]. Too small a speckle grain size would therefore preserve and even enhance the nonmonotonic evolution of the image acquisition performance with the speckle noise level. Alternatively, too large a speckle grain size would not modify the speckle noise distribution but would impose a larger sensor CCD matrix in order to preserve similar efficacy in the estimation of the statistical averages, as in Fig. 1. Also, in the speckle noise model of Eq. (14), a single standard deviation  $\sigma$  is assumed for the speckle over the whole image  $N(u, v)$ . Therefore, special attention has to be devoted to control experimentally the uniformity of the laser beam. In our case, this is ensured by a spatial filter designed to obtain a clean laser beam quasiuniform around its center, covering the CCD matrix. Experimental results produced by the setup described above are also presented in Fig. 1 for comparison with the theoretical predictions. The results of Figs. 1(A) and 1(B) demonstrate, under the conditions indicated, a good agreement with the theoretical calculation of the performance measures  $C_{SY}$  and  $Q_{SY}$ .

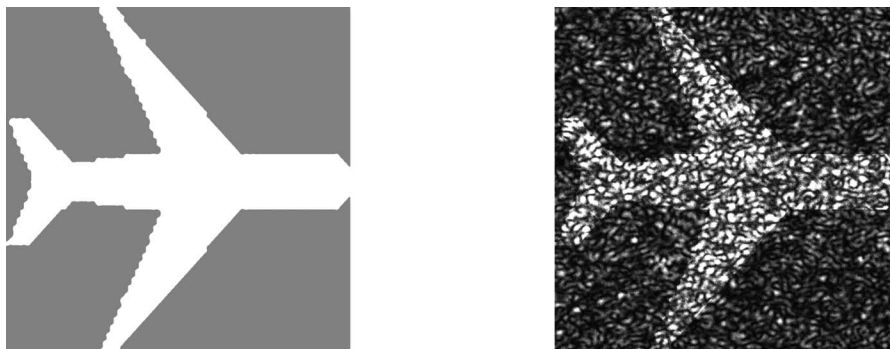


Fig. 2. (Left) Input image  $S(u, v)$ , with size  $1024 \times 1024$  pixels, used for the experimental validation presented in Fig. 1, where the object is occupying  $p_1=27\%$  of the image surface and parameters  $I_0=0.5$ ,  $I_1=1.5$ . (Right) Corresponding intermediate image  $X(u, v)$  obtained with a speckle noise rms amplitude  $\sqrt{2}\sigma=0.42$ .

## 7. INTERPRETATION

Figure 1 illustrates how an image can be acquired with maximum efficacy when a sufficient amount of speckle noise is injected in the present coherent imaging system. This feature can be interpreted as a form of stochastic resonance or a useful-noise effect. Stochastic resonance is an *a priori* counterintuitive phenomenon in a purely linear context, and it generally requires the presence of a nonlinear system in order to occur. The nonlinearity here is the saturating part in the response of the image acquisition device. As depicted in Fig. 3, at the optimal level of speckle noise, the saturation of the acquisition device affects almost only the pixels of one of the two regions (background and object) of the image. In Fig. 3, since  $I_1 > I_0$ , the pixels saturated in the acquired image  $Y(u, v)$  almost all belong to the object region. Therefore, under the optimal speckle noise conditions of Fig. 3, the object region in the acquired image is somehow denoised by the saturation of the acquisition device. For too low a level of speckle noise, the acquired image is not saturated at all and cannot benefit from this denoising by saturation. For too high a level of the speckle noise, saturation progressively affects both regions of the acquired image, which loses its contrast and thus its similarity with the input binary image  $S(u, v)$ . This provides a qualitative interpretation for the nonmonotonic evolutions of the performance measures quantified in Fig. 1 when the level of the speckle noise is raised.

Based on the results of [9], it can be expected that the possibility of a beneficial exploitation of speckle noise in the presence of saturation will carry over to images with distributed gray levels. In essence, the effect is not critically dependent on the discrete binary nature of the information-carrying signal. In general terms, the starting point is an information-carrying signal at a given initial level of noise that places the sensor to operate essentially in the linear part of its input–output characteristic. Then, from this point, a sufficient increase in the level of

noise at the input causes the sensor to operate in the saturation part of its response. As explained below, the saturation implements a clipping mechanism that has the ability to reduce the noise. With adequate control, this can lead to a situation at the output of the clipping device that is more favorable for the information-carrying signal than its initial situation with no clipping. The feasibility of such an effect was shown in [9] for continuously distributed 1D temporal signals with additive noise. Here we have demonstrated the feasibility of the effect on binary 2D spatial signals (images) with multiplicative speckle noise.

## 8. CONCLUSION

For coherent imaging, we have demonstrated that saturation of an acquisition device can be exploited to perform a signal transmission more efficient than that of a purely linear sensor. Optimal transmission is obtained by adjusting the speckle noise at a sufficient level, which deliberately operates the acquisition device in its saturating part. This constructive action of speckle noise cooperating with saturation is interpreted as a novel instance of stochastic resonance. The possibility of a constructive action of the multiplicative speckle noise has been illustrated with an exponential speckle probability density and binary images. Under these conditions, we have shown good agreement between theoretical and experimental results in relation to influence of speckle noise grain size. A qualitative explanation of the mechanism at the root of the improvement by the speckle noise has also been proposed. It appears in this way that, with binary images buried in speckle noise, clipping in the acquired images can be a useful operation that acts as a denoising stage, which can be, as demonstrated here, optimally controlled by tuning the speckle noise at a sufficient level. Because of the practical importance of saturating sensor characteristics, this result constitutes an interesting extension of [8], where

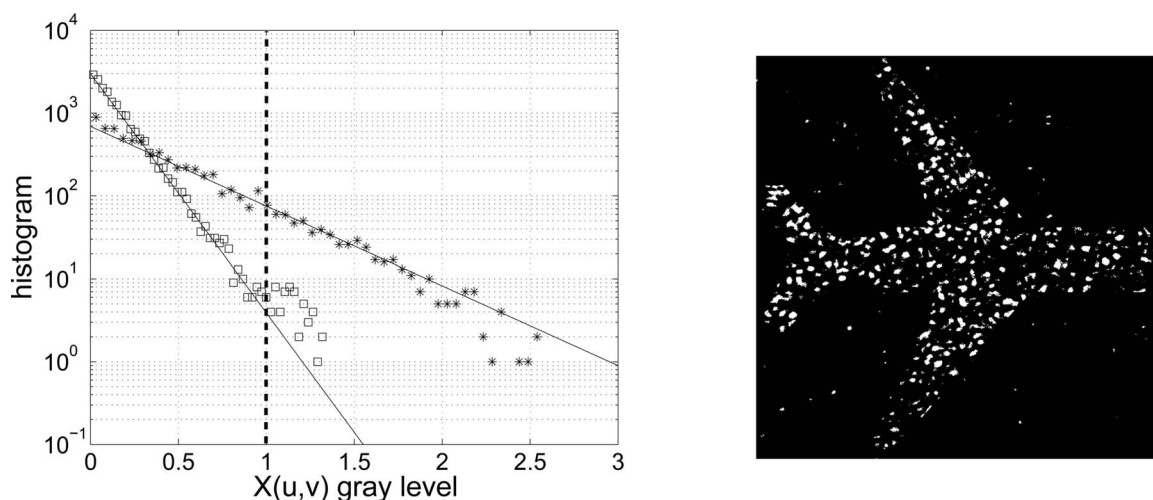


Fig. 3. (Left) Histogram of background ( $\square$ ) and object ( $*$ ) regions in intermediate image  $X(u, v)$  of Eq. (1) on a logarithmic scale. Input image  $S(u, v)$  is the same as in Fig. 2 (left). The solid curves are the theoretical histograms calculated from the exponential model of Eq. (14). The dashed curve stands for the saturating level  $\theta=1$  of the acquisition image device. Speckle noise is obtained from the experimental setup of [8] with an rms amplitude  $\sqrt{2}\sigma=0.42$ , corresponding to the optimal value of normalized cross covariance  $C_{SY}$ . (Right) Binary image representing only the pixel saturated in the acquired image  $Y(u, v)$  under the acquisition conditions of the left panel of this figure.

the possibility of nonmonotonic evolutions of image acquisition performance as a function of the speckle noise amplitude was shown with a simple 1-bit quantizer.

Acquisition, usually seen as the very first step in an information processing chain, is conventionally designed to reproduce a faithful representation of the physical signal with the highest linear fidelity. Here we have shown how the nonlinear saturating part of an acquisition device can also be used as a preprocessor capable of denoising properties usually undertaken at higher levels in the information processing chain. Comparable situations where the clipping effect of a saturating device can benefit from the processing of an information-carrying signal can also be found in other contexts. In signal detection [12], the effect can be used to reduce the detrimental impact on the performance of detectors of spikes due to non-Gaussian heavy-tailed additive noises. Some distinct nonlinear effects, bearing some similarity with the present clipping effect, have also been reported in other areas of coherent imaging [13–15]. Some benefits of clipping are shown in [13–15] for real-time image processing. Yet in these references, the clipping that is used is meant as hard clipping, which is, in fact, a 1-bit quantization of the image. This differs in essence from the type of clipping we consider here, arising from the linear response of a sensor that reaches saturation. Moreover, the processes addressed in [13–15] are postacquisition processes distinct from the acquisition task investigated here at the sensor level.

Results of this report could be extended in several directions. For example, more sophisticated images with distributed gray levels, instead of binary images, could be tested. The case of coherent images with distributed gray levels can be investigated by means of the general theoretical framework developed here, which is valid for any type of speckle noise and input image distribution. As discussed in Section 7, the stochastic resonance or useful-noise effect reported here is expected to carry over to images containing more than two gray levels. Therefore, it would be interesting to confront, as done here, theoretical and experimental results and to examine how the beneficial action of speckle noise in association with saturation evolves in these other conditions of coherent imaging. One could also consider image processing tasks other than the acquisition task treated here. Image processing techniques for coherent imaging that take into account the statistical properties of the noisy images are commonly implemented, for instance, for detection [16], segmentation [17], or parameter estimation [18] purposes. These techniques usually assume a perfectly linear model for the acquisition device, and the experimental images acquired for the validation of their theoretical performance are made at a low level of speckle noise to minimize the saturation that always exists in practice. Therefore, it would be interesting to investigate the performance of

such detection, segmentation, or parameter estimation techniques as described in [16–18], with the presence of a saturating part in the response of the acquisition device, and in the light of the present results that predict an increased benefit that can be drawn from saturation.

## REFERENCES

1. L. Gammaitoni, P. Hänggi, P. Jung, and F. Marchesoni, "Stochastic resonance," *Rev. Mod. Phys.* **70**, 223–287 (1998).
2. F. Chapeau-Blondeau and D. Rousseau, "Noise improvements in stochastic resonance: from signal amplification to optimal detection," *Fluct. Noise Lett.* **2**, 221–233 (2002).
3. B. M. Jost and B. E. A. Saleh, "Signal-to-noise ratio improvement by stochastic resonance in a unidirectional photorefractive ring resonator," *Opt. Lett.* **21**, 287–289 (1996).
4. F. Vaudelle, J. Gazengel, G. Rivoire, X. Godivier, and F. Chapeau-Blondeau, "Stochastic resonance and noise-enhanced transmission of spatial signals in optics: the case of scattering," *J. Opt. Soc. Am. B* **15**, 2674–2680 (1998).
5. K. P. Singh, G. Ropars, M. Brunel, and A. Le Floch, "Stochastic resonance in an optical two-order parameter vectorial system," *Phys. Rev. Lett.* **87**, 213901 (2001).
6. F. Marino, M. Giudici, S. Barland, and S. Balle, "Experimental evidence of stochastic resonance in an excitable optical system," *Phys. Rev. Lett.* **88**, 040601 (2002).
7. K. P. Singh, G. Ropars, M. Brunel, and A. Le Floch, "Lever-assisted two-noise stochastic resonance," *Phys. Rev. Lett.* **90**, 073901 (2003).
8. S. Blanchard, D. Rousseau, D. Gindre, and F. Chapeau-Blondeau, "Constructive action of the speckle noise in a coherent imaging system," *Opt. Lett.* **32**, 1983–1985 (2007).
9. D. Rousseau, J. Rojas Varela, and F. Chapeau-Blondeau, "Stochastic resonance for nonlinear sensors with saturation," *Phys. Rev. E* **67**, 021102 (2003).
10. F. Chapeau-Blondeau, S. Blanchard, and D. Rousseau, "Noise-enhanced Fisher information in parallel arrays of sensors with saturation," *Phys. Rev. E* **74**, 031102 (2006).
11. J. W. Goodman, *Speckle Phenomena in Optics* (Roberts & Company, 2007).
12. S. Kay, *Fundamentals of Statistical Signal Processing: Detection Theory* (Prentice Hall, 1998).
13. J. Ohtsubo and A. Ogiwara, "Effects of clipping threshold on clipped speckle intensity," *Opt. Commun.* **65**, 73–78 (1988).
14. A. Ogiwara, H. Sakai, and J. Ohtsubo, "Real-time optical joint transform correlator for velocity measurement using clipped speckle intensity," *Opt. Commun.* **78**, 322–326 (1990).
15. R. H. Sperry and K. J. Parker, "Segmentation of speckle images based on level-crossing statistics," *J. Opt. Soc. Am. A* **3**, 490–498 (1991).
16. F. Goudail, P. Réfrégier, and G. Delyon, "Bhattacharyya distance as a contrast parameter for statistical processing of noisy optical images," *J. Opt. Soc. Am. A* **21**, 1231–1240 (2004).
17. F. Goudail and P. Réfrégier, *Statistical Image Processing Techniques for Noisy Images* (Kluwer, 2004).
18. P. Réfrégier, J. Fade, and M. Roche, "Estimation precision of the degree of polarization from a single speckle intensity image," *Opt. Lett.* **32**, 739–741 (2007).